Facile Fabrication of Electrospun Nanofibrous Aerogels for Efficient Oil Absorption and Emulsified Oil−Water Separation

Guojun Jiang, Caidan Zhang,* Sheng Xie, Xiaohong Wang, Weiwei Li, Jiajie Cai, Fei Lu, Yuhang Han, Xiangyu Ye, and Lixin Xue

Read Online

ACCESS | Metrics & More | Article Recommendations | Supporting Information

ABSTRACT: Developing superabsorbents for efficiently separating immiscible oil−water mixtures and oil−water emulsions are highly desirable for addressing oily wastewater pollution problems, but it remains a challenge. Ultralight nanofibrous aerogels (NFAs) with unique wetting properties show great potential in oily wastewater treatment. In this study, a facile and efficient method for producing hierarchical porous structured NFAs with hydrophobicity for high efficiency oil−water separation was developed. The synthesis included three steps: wet electrospinning, freeze drying, and in situ polymerization. The obtained NFA demonstrated outstanding oil absorption capacity toward numerous oils and organic solvents, as well as efficient surfactant-stabilized water-in-oil emulsion separation with high separation flux and excellent separation efficiency. Furthermore, these NFAs displayed excellent corrosion resistance and outstanding recoverability. We assume that the resultant NFAs fabricated by this facile strategy are highly promising as ideal oil absorbents for practical oily wastewater treatment under harsh conditions.
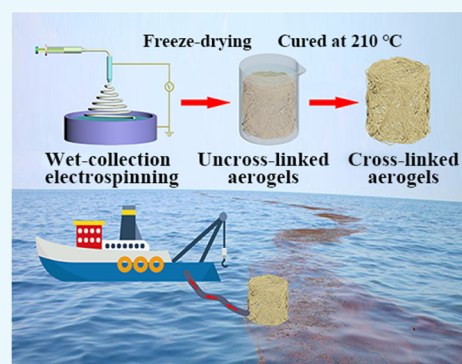
1. INTRODUCTION

Over the years, oily wastewater from oil spills, oily domestic sewage, and industrial chemical leakages has become a global threat to our living environment and ecosystems.[1−3] Therefore, the efficient treatment of oily wastewater has become an urgent global challenge. To address this issue, considerable efforts have been made to develop several advanced technologies and materials for oily wastewater remediation, such as chemical method,[4] physical method (absorbent materials[5,6] and skimming[7]), bioremediation,[8,9] and in situ burning.[10] Among these alternatives, the absorption method based on three-dimensional (3D) absorbent materials is considered the most attractive and effective approach because of its low cost, convenience, and efficiency. Furthermore, the absorbed oils and organic solvents can be recycled simply by mechanical squeezing. Typically, an ideal oil absorbent material for oil−water separation is expected to possess a high oil-absorbing capacity, excellent oil−water selectivity, good chemical stability, low cost, easy fabrication, and superior recyclability.

Aerogels have piqued the interest of many researchers and are extensively investigated as oil−water separation materials because of their intriguing properties, such as low density, high porosity, high specific surface areas, and adjustable surface chemistry. Recently, several types of aerogels with special wettability, such as traditional inorganic, synthetic, and natural polymer aerogels, have been commonly designed for separating of oil−water mixtures. However, traditional silica aerogels are

susceptible to mechanical brittleness and poor recovery, limiting their practical application in oily wastewater treatment. Some synthetic polymer aerogels have improved mechanical properties and reusability, but many shortcomings, such as low oil sorption capacity and hydrophobicity, limit their commercial application. For sustainable bio-aerogels, such as cellulose aerogels (natural cellulose ones,[11] regenerated cellulose ones,[12] and cellulose-derivate ones[13]), chitosan,[14] gelatin,[15] wood,[16] and marine algae,[17] the separation efficiency and mechanical robustness are low. Simultaneously, carbon-based aerogels, such as carbon nanotubes,[18] carbon fibers,[19] graphene,[20] and the corresponding composite aerogels, demonstrate superior absorption capacities and recyclability.[21,22] However, some limitations remain, such as expensive raw materials, low efficiency, and complicated fabrication processes, which significantly limit their practical applications. These limitations in existing aerogels have prompted many researchers to explore advanced oil absorbents with superior absorption capacity, high selectivity, reusability, and low cost.

Alternatively, nanofibrous aerogels (NFAs) with a highly open hierarchical structure and extremely low-energy surface have been extensively investigated and show tremendous potential for selective oil absorption and oil−water mixture separation. For example, Ding et al. first presented a robust methodology to create superelastic and superhydrophobic polyacrylonitrile (PAN)/SiO_2 hybrid NFAs with extremely high flux (maximum of 8140 ± 220 L·m^{-2}·h^{-1}) and separation efficiency (over 99.995%).[23] Similarly, Fong et al. developed an innovative approach for designing ultralight electrospun cellulose sponges, which demonstrated a super-high oil absorption capacity of up to 270 times its original weight, mechanical robustness, and excellent chemical stability.[24] Following that, Xiao et al. prepared thermoplastic polymer EVOH NFAs using a facile freeze-drying process, achieving an absorption capacity of up to 102 times their weight, superior mechanical elasticity, and excellent recyclability.[25] Recently, Deng et al. demonstrated a simple method to design superelastic and robust SiNFs/PI-NFAs with excellent absorption capacity (70−159 g g^{-1}) and effectively separate water-in-oil emulsions.[26] In a previous study, our group successfully prepared polydimethylsiloxane (PDMS)-functionalized PAN@PDMS NFAs using coaxial electrospinning and solution immersion methods, respectively. The resulting aerogels showed excellent absorption performance (55.43−127.37 g g^{-1}), superior chemical stability, excellent recyclability, and outstanding separation efficiency (above 99.47 wt %).[27,28] These studies provide a novel approach for the design and development of efficient aerogels for oil absorption and oil−water separation. However, these reported fabrication processes of NFAs are typically complicated and time-consuming. Therefore, developing an innovative approach for convenient fabrication of highly hydrophobic/oleophilic NFAs with high performance on oil−water separation is of great significance.

In this study, we reported a versatile and feasible approach to fabricate ultralight NFAs through simple directional liquid-assisted collection electrospinning, freeze-drying, and in situ polymerization processes, which eliminate a time-consuming homogenization step in the traditional NFAs' synthesis process. The obtained NFAs have a self-assembled hierarchical structure with an ultralow apparent density. In addition, they possess high hydrophobicity and superoleophilicity, demonstrating superabsorbent properties in separating oil from layered and emulsified oil−water mixtures. Moreover, they also have outstanding mechanical stability, excellent chemical stability, and excellent absorption recyclability. It is assumed that this study will open new avenues for designing and developing an advanced absorbent material for environmental protection.

2. RESULTS AND DISCUSSION

2.1. Preparation and Morphological Characterization of PBA/PAN NFAs.
Figure 1a shows the facial fabrication process of poly butyl acrylate (PBA)/PAN NFAs. In summary, the formation of PBA/PAN NFAs can be divided into three stages, namely, wet electrospinning, freeze-drying, and thermal treatment. The electrospun nanofibers were deposited loosely on the liquid surface during the wet electrospinning process to form a nonwoven layer. Notably, the surface tension of the collecting liquid was critical for ensuring liquid penetration into the interspace of the nanofibrous network, resulting in the spontaneous formation of a 3D nanofibrous matrix with loose
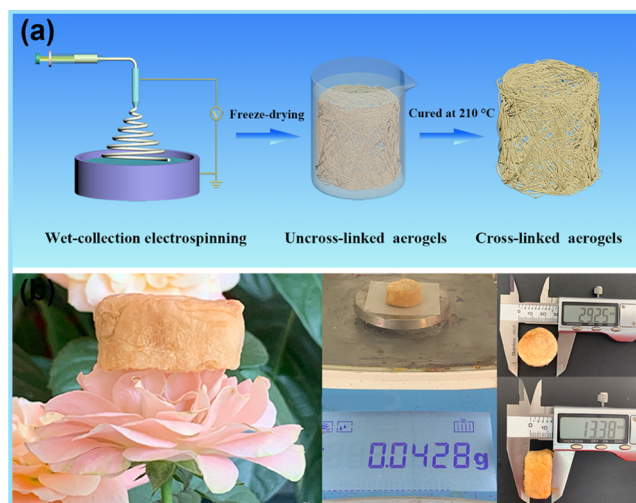

Figure 1. (a) Schematic illustration of the preparation of the PBA/PAN NFAs. (b) PBA/PAN NFA on top of a flower, indicating low weight.

structures. Water/t-BuOH (1:1, v/v) with low surface tension was chosen as the collecting liquid to effectively decrease the surface tension of the collecting liquid and prevent nonsolvent evaporation during the wet electrospinning process. Furthermore, the 3D nanofibrous matrix was immediately transferred into 3D molds and rapidly freeze-dried to self-assemble into uncross-linked NFAs. Finally, the prepared uncross-linked NFAs were thermally cured. Notably, the thermal curing treatment was critical for ensuring the structural stability of the PBA/PAN NFAs against external stress and remarkable hydrophobicity even under extremely harsh conditions. Meanwhile, the loosely packed 3D PBA/PAN NFA can easily stand on top of a flower (Figure 1b), indicating its ultralight feature.

Scanning electron microscopy (SEM) was used to characterize the microstructures and morphologies of the as-prepared 3D PBA/PAN NFAs with varying densities. In striking contrast with previous studies that have found that the conventional NFAs showed hierarchical cellular architectures, the as-obtained NFAs demonstrated significant lamellar structures, with densely packed nanofibers on the layer, whereas sparse nanofibers fill the spaces between nanofiber layers (Figure 2). Typical cross-sectional SEM images of all NFAs revealed a dual porous microstructure, with lamellar structures (few tens to few hundred micrometers) generated by ice crystal sublimation and slender pores (smaller than 2 μm) generated by the self-assembly of nanofibers. Tuning the density of the NFA can be used to control the interlayer distance. The interlayer distance decreased as the electrospinning depositing time increased from 30 to 90 min (Figure 2). Note that this specific hierarchical porous structure combined the advantages of both NFAs (ultrahigh porosity) for oil storage and electrospun nanofibrous membranes (random accumulation of nanofibers) for emulsion separation.

2.2. Mechanical Properties of the As-Prepared PBA/PAN NFAs.
To achieve high reusability in practical recycling applications, excellent mechanical performance is required. The influence of density on the mechanical properties of as-prepared PBA@PAN NFAs was evaluated using compressive stress−strain ($\sigma-\varepsilon$) curves (Figure 3). During the compression loading process, these curves displayed two typical character-
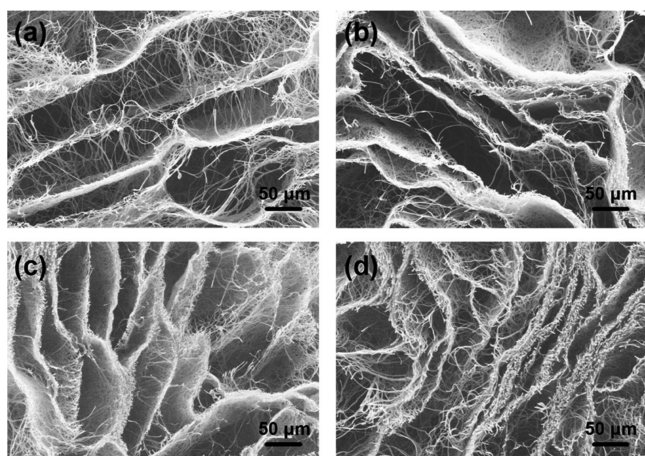
Figure 2. Microscopic architecture of the PBA@PAN NFAs obtained with various densities: (a) PBA/PAN-30, (b) PBA/PAN-50, (c) PBA/PAN-70, and (d) PBA/PAN-90.

istic regimes of open honeycomb-like foams: an initial linear Hookean regime under low compressive strain (ε less than 35%), corresponding to the bending of nanofibers and gradual deformation of pores; and a densification regime under high compressive strain (ε greater than 35%), corresponding to the densification of pores.[29] The compressive stress−strain curves of PBA@PAN NFAs with different densities were obtained under various strains of 20, 40, and 60% (Figure 3a−d). The density of the NFAs had a significant effect on compressive behavior. The results showed that the maximum compressive strength significantly increases as the densities of the PBA@PAN NFA increase from ∼4.79 to ∼11.21 mg cm^{-3}. However, when the density exceeded ∼11.21 mg cm^{-3}, the maximum compressive strength of NFA did not improve the compressive strength. This is mainly because the nanofiber layers were densely packed as the density of the NFAs increased, resulting in improved mechanical performance. After releasing the compression loading, the PBA@PAN NFA can instantly recover to its original shape, demonstrating outstanding
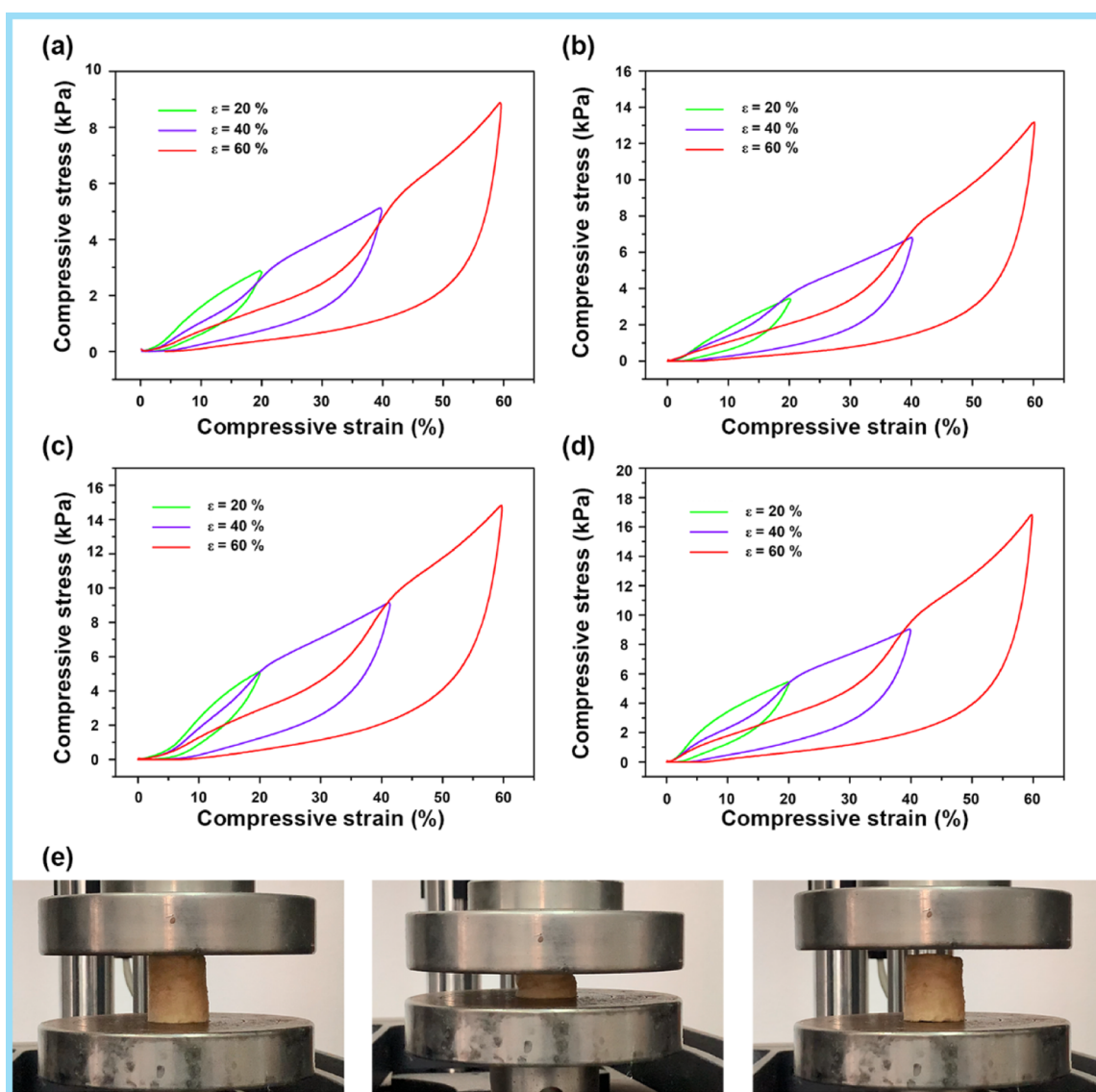
Figure 3. Compressive stress−strain curves of different PBA/PAN NFAs: (a) PBA/PAN-30, (b) PBA/PAN-50, (c) PBA/PAN-70, (d) PBA/PAN-90, and (e) photographs of PBA/PAN-70 under compression and release ($\varepsilon = 60\%$).
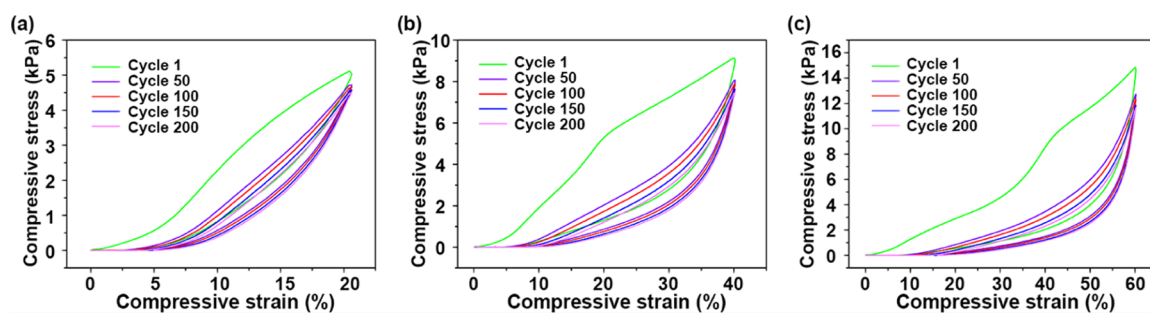
Figure 4. Cyclical performance of PBA/PAN-70 undergoing compression and release for 200 cycles with (a) 20, (b) 40, and (c) 60% of strain.
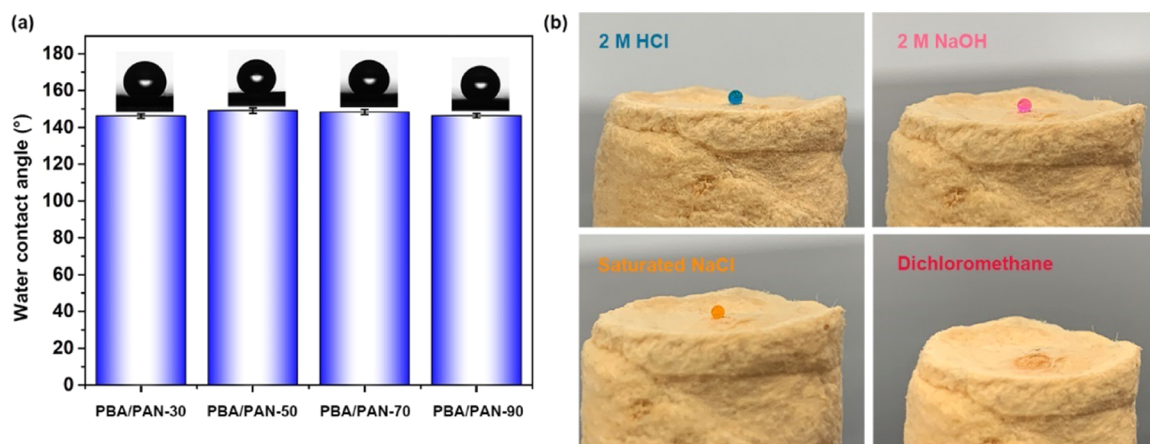

Figure 5. (a) Water contact angle of different PBA/PAN NFAs. (b) Digital pictures showing the state of different liquid droplets on the surface of PBA/PAN-70.
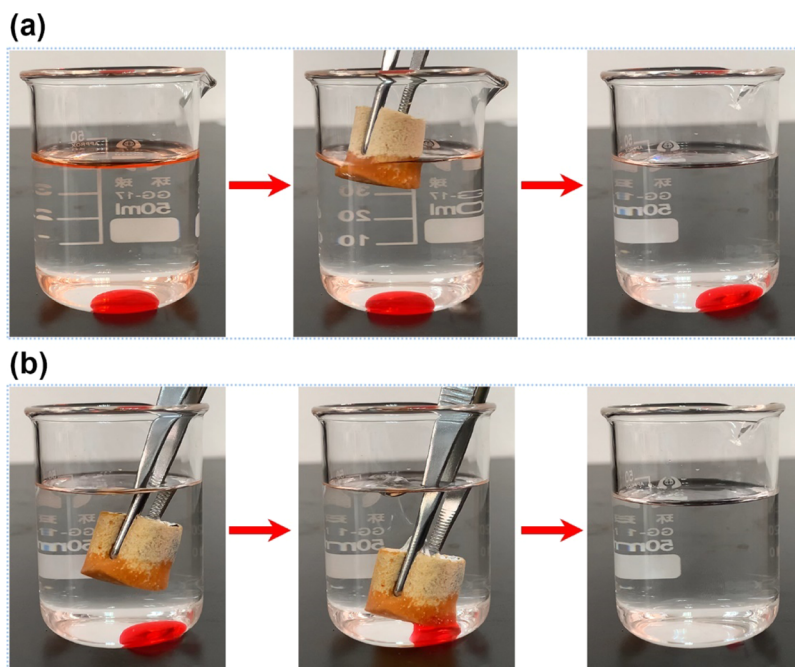

Figure 6. Organic solvent absorption performances of PBA/PAN-70. (a) Removal of *n*-hexane floating on the surface of the water. (b) Removal of chloroform at the bottom of the water.

mechanical properties for large deformations without fracture or collapse (Figure 3e).

Furthermore, PBA@PAN NFAs with a density of ∼11.21 mg cm^{-3} were subjected to cyclic compressive stress−strain tests under different strains of 20, 40, and 60%, which

demonstrated excellent compressive recovery capability (Figure 4). Similar to other resilient cellular materials, hysteresis loops and plastic deformation in the hysteresis curves were observed after repeated compression, indicating energy dissipation.[25] PBA@PAN NFAs showed slight plastic
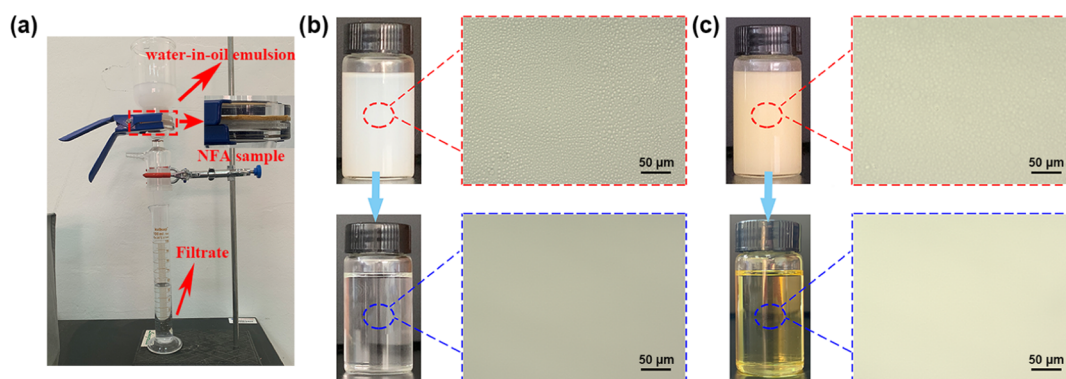
Figure 7. Optical microscopy images of water-in-oil emulsion before and after filtration by PBA/PAN-70 (a). Setup for water-in-oil emulsion separation, (b) water-in-*n*-hexane, and (c) water-in-peanut oil.

deformation (4.8% at 20% strain, 10.2% at 40% strain, and 14.6% at 60% strain) after 200 fatigue cycles, which is much lower than many polymeric foams and most existing fibrous sponges (more than 20% at 60% strain).[26] Meanwhile, after 200 cyclic compressions, the PBA@PAN NFAs showed no significant reduction in mechanical strength, indicating that they can retain more than 85% of the maximum compressive stress at the 50th cycle and they tend to be stable over the next 150 compressive loading—unloading cycles, clearly indicating their structural robustness during cyclic compression. These superior mechanical properties can be attributed mainly to the PBA@PAN NFA's unique lamellar structure. Benefiting from the excellent compressive properties, PBA@PAN NFA is promising for use as recyclable absorbents in practical applications.

2.3. Surface Wetting Behavior of the As-Prepared PBA/PAN NFAs. Water contact angle (WCA) was measured as an important indicator for assessing the selective absorption of oils and organic solvents from water. WCA measurements were used to characterize the surface wettability of the PBA/PAN NFAs, and the effect of density on the WCA is shown in Figure 5a. According to the Wenzel and Cassie—Baxter models, surface wettability is strongly influenced by surface roughness and surface energy.[30] The WCA values of the as-prepared PBA/PAN NFAs are above 140° because of the rough surface structure of the NFAs and the low surface energy of polybenzoxazine. As assumed, the WCA of the PBA/PAN NFAs did not differ significantly, demonstrating that the density of the NFAs had no significant effect on the WCA. Additionally, corrosive liquids, such as strong acid (2 M HCl), alkali (2 M NaOH), and saturated NaCl, can maintain a full spherical shape on the PBA/PAN NFA surface. However, the oil droplets are spread on the surface and are immediately immersed in the NFA, indicating that the as-prepared PBA/PAN NFAs have robust hydrophobicity and lipophilicity in different corrosive environments (Figure 5b). The above phenomena demonstrate promising applications of PBA/PAN NFAs in the field of oil—water separation.

The as-prepared PBA/PAN NFAs can be used as ideal absorber materials for selectively removing oil pollutants from wastewater because of their hierarchical porous structure, excellent compression recoverable properties, and highly hydrophobic/oleophilic surfaces. As assumed, the obtained PBA/PAN NFAs demonstrated excellent selective absorption for different oils (light oil and heavy oil) from water. The as-prepared PBA/PAN NFA can completely absorb light oils

floating on the water's surface (*n*-hexane, stained with Sudan red III) and heavy oils underwater (dichloromethane, stained with oil red) within a few seconds, resulting in transparent and clean water (Figure 6). Notably, the as-prepared PBA/PAN NFA was not wetted by water and can hold absorbed oily liquids without any liquids release throughout the separation process, confirming that PBA/PAN NFA has excellent oil-water selectivity.

2.4. Oil and Organic Solvent Absorbency of the As-Prepared PBA/PAN NFAs. Based on the above-mentioned results, various common pollutants in our daily lives and chemical industries, including *n*-hexane, gasoline, diesel, peanut oil, dichloromethane, and chloroform were used in a separation test to investigate the absorption performance of the as-prepared PBA@PAN NFAs with varying densities. The as-prepared PBA@PAN NFAs with a density of ~4.79 mg cm^{-3} demonstrated a significant absorptive capacity toward these oils and organic solvents (see Supporting Information, Figure S1a), ranging from 101.92 to 268.27 times its weight, depending on the density of the liquids. This could be associated with the extremely low density and high porosity of the NFAs. However, as the density of the NFA increased, the absorption capacity of the PBA@PAN NFAs decreased significantly. Particularly, PBA@PAN NFAs with a density of ~15.12 mg cm^{-3} demonstrated absorption capacities ranging from 33.08 to 98.25 times their weight. The difference in adsorption capacities is because the NFAs with low density had larger lamellar porous structures inside, which can provide more space for oil storage. As previously discussed, increasing the density of the NFA can decrease the interlayer distance, decreasing porosity. Nevertheless, the as-prepared PBA@PAN NFAs had a much higher absorption capacity than many previously reported absorbing materials.[31,32]

Besides the absorption capacity, the recyclability and reusability of the absorbent material were also important criteria for evaluating its performance in practical applications. The recyclability of NFAs was determined using a simple cyclic adsorption-squeezing test, which was repeated 50 times for convenience and practicality. The density had a significant impact on the recyclability of the NFA (see Supporting Information, Figure. S1b). After 50 recycles, NFA with higher density could maintain a stable sorption and recycling performance, as well as retain more than 90% of its original capacity. However, NFA with low density is maintained with the range of 37.34−63.98% of its original capacity, indicating poor stability and durability. This could be attributed to

distinct differences in compressive stress. The results of the above mechanical testing show that NFA with higher density displayed higher compressive stress, which could provide high structural strength against pore deformation during the cyclic adsorption-squeezing tests. Thus, it is assumed that NFA with higher density could maintain a stable liquid sorption capacity, especially for liquid with high viscosity.

2.5. Emulsion Separation Performance of the As-Prepared PBA/PAN NFAs. Besides efficient adsorption performance in the separation of immiscible oil−water mixture, treating surfactant-stabilized emulsions is more difficult because of their higher stability and microscale dimensions (dispersed phase < 20 μm). Based on the results obtained thus far for different NFA samples, NFAs with a density of ∼11.21 mg cm^{-3} were chosen to further evaluate the emulsion separation performance. Therefore, several surfactant-stabilized water-in-oil emulsions, such as water-in-*n*-hexane, water-in-dichloromethane, water-in-petroleum ether, and water-in-peanut oil, were prepared to assess the oil-water emulsion separation performance of the as-prepared NFAs. After separation, the original feed milky emulsions successfully turned to a transparent oil phase (Figure 7), and the optical microscope images presented numerous water droplets dispersed throughout the feed emulsion, whereas nearly no visible water droplets were observed in the filtrate. These results confirmed that the as-prepared PBA/PAN NFAs can successfully separate water-in-oil emulsions. Furthermore, the flux and separation efficiency of the NFAs in various water-in-oil emulsions were evaluated. The emulsions demonstrated high flux directed only by gravity (1829 ± 48, 1716 ± 41, and 1792 ± 38 L·m^{-2}·h^{-1} for water-in-*n*-hexane, water-in-dichloromethane, and water-in-petroleum ether, respectively), except for that of the water-in-peanut oil emulsions (32 ± 3 L·m^{-2}·h^{-1}) (Figure 8). The differences in the flux of various water-in-
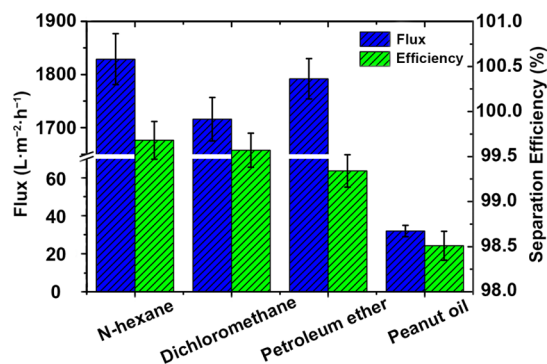
Figure 8. Flux and separation efficiency of PBA/PAN-70 in various water-in-oil emulsions.

oil emulsions could be explained by the differences in viscosity, which is inversely proportional to the flux of water-in-oil emulsion.[33] When the emulsion permeated through the NFA, the increased viscosity created more resistance to permeation, resulting in a lower filtrate flux. Furthermore, the as-prepared NFAs showed high separation efficiency of more than 99.6% for various surfactant-stabilized water-in-oil emulsions. This can be explained by the excellent hydrophobicity/lipophilicity of the NFAs, hierarchical porous channels inside the NFAs, and membrane structure of the nanofiber layers.

3. CONCLUSIONS

In summary, we have developed a facile and efficient method for producing PBA/PAN NFAs with hierarchical porous structures for highly efficient oil absorption and emulsion separation. The as-prepared PBA/PAN NFAs showed ultralow density (4.79−15.12 mg cm^{-3}), outstanding reversible compressibility (stress retention above 85% after 200 cycles), excellent hydrophobicity/lipophilicity (with a water contact angle of 149.1° and an oil contact angle of 0°), ultrahigh oil absorption capacity (especially up to 268.27 g g^{-1} for chloroform) toward various oils and organic solvents, and remarkable chemical stability under harsh conditions (e.g., 2 M NaOH, 2 M HCl, and salty environments). Furthermore, the as-prepared PBA/PAN NFAs demonstrated efficient surfactant-stabilized water-in-oil emulsion separation performance with high emulsion permeation fluxes (1716 ± 41 L·m^{-2}·h^{-1}) and high separation efficiency (above 99.6 wt %). Considering the aforementioned benefits, the as-prepared PBA/PAN NFAs developed in this study are assumed to achieve desirable applications in the practical treatment of various oily wastewaters discharged from industry and our daily lives.

4. EXPERIMENTAL SECTION

4.1. Materials. Polyacrylonitrile (M_w = 85,000 g/mol) was purchased from the Shanghai Chemical Fibers Institute. The benzoxazine (BA) monomer was synthesized and purified using the previously reported methods.[34] Hydrochloric acid (HCl), sodium hydroxide (NaOH), Oil Red, Sudan Red III, span 80, *N,N*-dimethylformamide (DMF), *tert*-butanol (*t*-BuOH), *n*-hexane, gasoline, diesel, peanut oil, dichloromethane, chloroform, petroleum ether, and other chemicals were purchased from Macklin Chemical Industry Co., Ltd., China. All chemicals were of analytical grade and were used as received.

4.2. Preparation of PBA/PAN NFA. First, the BA/PAN mixed solution was obtained by dissolving PAN and BA powder in DMF using magnetic stirring for 8 h to obtain a transparent solution with a concentration of 14 wt %, and the weight ratio of BA to PAN was 1:10. Subsequently, the wet electrospinning process was performed on a standard electrospinning apparatus (Shenzhen Tongli Weina Technology Co. Ltd., China), and a liquid vessel (water/*t*-BuOH = 1:1 v/v) was used as the collector. The flow rate of the BA/PAN solution was set to 0.6 mL h^{-1}. The distance from the spinneret to the surface of the collecting liquid was maintained at 15 cm, and the applied voltage on the spinneret was fixed at 22 kV. The temperature and relative humidity inside the electrospinning chamber was 25 ± 2 °C and 65 ± 5%, respectively. After completing the electrospinning process at a specific time, the obtained BA/PAN nanofibrous dispersion was transferred into the designed molds to shape them as cylinders and frozen using liquid nitrogen. Then, the frozen samples were vacuum freeze-dried for 48 h inside a lyophilizer (SJIA-12 N, Ningbo SJIA Instrument Co., Ltd, China) under a pressure of 5 Pa to obtain uncross linked BA/PAN NFAs. Finally, these uncross-linked BA/PAN NFAs were cured in a vacuum oven at 210 °C for 2 h to obtain robust PBA/PAN NFAs. Note that the densities of the NFAs can be easily manipulated by controlling the electrospinning time and volume of the designed mold. The obtained PBA/PAN NFAs depending on the electrospinning time (min) were denoted as PBA/PAN-30, PBA/PAN-50, PBA/PAN-70, and

PBA/PAN-90, with densities of ~4.79, ~8.13, ~11.21, and ~15.12 mg/cm^3, respectively.

4.3. Characterization Methods and Measurements.

SEM (Hitachi S-4800, Japan) was used to characterize the microscale morphologies of the as-prepared aerogels. A contact angle analyzer (OCA20, DataPhysics Instruments, Germany) was used to measure the wettability at room temperature using a water droplet (6 μL) as an indicator. The compressive behavior was performed on using a universal testing machine (CMT4304, Shenzhen SANS Test Machine Co. Ltd., Shenzhen, China) equipped with a load cell of 50 N at room temperature. The stress−strain curves at ε = 20, 40, 60% and loading-unloading fatigue cyclic compressive tests were measured at a loading rate of 100 mm min^{-1}. The bulk density of the NFAs was determined by dividing their mass by its geometric volume. A Karl Fischer moisture titrator (MKS-500, Japan) was used to determine the water contents in the original emulsions and the corresponding collected oil filtrates. Optical microscopy images were recorded using an optical microscope (Olympus BX53, Japan) after placing a drop of the emulsion onto a transparent glass board.

The absorption capacities of the NFAs for various oils and organic solvents (including *n*-hexane, gasoline, diesel, peanut oil, dichloromethane, and chloroform) were also evaluated using the following method. Typically, NFA samples were extracted after being submerged in different types of oils or organic solvents for 2 min to achieve equilibrium and then allowed to drain for another 30 s. The absorption capacity of the NFAs (Q) can be calculated according to eq 1

$$Q = (wt_{after} - wt_{before})/wt_{before} \qquad (1)$$

where wt_{after} is the weight of the wet sample at absorption equilibrium and wt_{before} is the weight of the dry sample.

The gravity driven oil/water separation performance of the NFAs (thickness of 5 mm) for various water-in-oil emulsions was assessed with a homemade filtration apparatus. The surfactant-stabilized water-in-oil emulsions were prepared by adding a certain amount of deionized water (1 wt %) into the oil (*n*-hexane, dichloromethane, petroleum ether, and peanut oil) with 0.1 wt % span 80 and stirring vigorously to form milky white solutions.

The fluxes (L·m^{-2}·h^{-1}) of the NFAs were calculated according to eq 2

$$flux = V/At \qquad (2)$$

where V represents the permeation volume, A is the cross-section area at the bottom of the glass tube, and t is the testing time.

The separation efficiency (E) was evaluated according to eq 3

$$E\ (\%) = (1 - C_f/C_0) \times 100\% \qquad (3)$$

where C_f and C_0 are water concentrations in the filtrate and the oil-water mixture, respectively.

■ ASSOCIATED CONTENT

⑤ Supporting Information

The Supporting Information is available free of charge at https://pubs.acs.org/doi/10.1021/acsomega.1c06080.

Oils/organic solvent absorption performance of different PBA/PAN NFAs (PDF)

■ AUTHOR INFORMATION

Corresponding Author

Caidan Zhang − *Key Laboratory of Yarn Materials Forming and Composite Processing Technology of Zhejiang Province, Jiaxing University, Jiaxing 314001, China;* ⊙ orcid.org/0000-0003-0307-3371; Email: caidanzhang@zjxu.edu.cn

Authors

Guojun Jiang − *Department of Science, Zhijiang College of Zhejiang University of Technology, Shaoxing 312000, China*

Sheng Xie − *Key Laboratory of Yarn Materials Forming and Composite Processing Technology of Zhejiang Province, Jiaxing University, Jiaxing 314001, China;* ⊙ orcid.org/0000-0002-0505-1988

Xiaohong Wang − *Department of Science, Zhijiang College of Zhejiang University of Technology, Shaoxing 312000, China*

Weiwei Li − *Department of Science, Zhijiang College of Zhejiang University of Technology, Shaoxing 312000, China*

Jiajie Cai − *Department of Science, Zhijiang College of Zhejiang University of Technology, Shaoxing 312000, China*

Fei Lu − *Department of Science, Zhijiang College of Zhejiang University of Technology, Shaoxing 312000, China*

Yuhang Han − *Department of Science, Zhijiang College of Zhejiang University of Technology, Shaoxing 312000, China*

Xiangyu Ye − *Zhejiang Light Industrial Products Inspection and Research Institute, Hangzhou 310020, China; Center for Membrane Separation and Water Science & Technology, College of Chemical Engineering, Zhejiang University of Technology, Hangzhou 310014, China*

Lixin Xue − *Center for Membrane Separation and Water Science & Technology, College of Chemical Engineering, Zhejiang University of Technology, Hangzhou 310014, China;* ⊙ orcid.org/0000-0002-1110-3684

Complete contact information is available at:
https://pubs.acs.org/10.1021/acsomega.1c06080

Notes

The authors declare no competing financial interest.

■ REFERENCES

(1) Su, R.; Li, S.; Wu, W.; Song, C.; Liu, G.; Yu, Y. Recent progress in electrospun nanofibrous membranes for oil/water separation. *Sep. Purif. Technol.* **2021**, *256*, 117790.

(2) Gupta, R. K.; Dunderdale, G. J.; England, M. W.; Hozumi, A. Oil/water separation techniques: a review of recent progresses and future directions. *J. Mater. Chem. A* **2017**, *5*, 16025−16058.

(3) Wei, Y.; Qi, H.; Gong, X.; Zhao, S. Specially Wettable Membranes for Oil-Water Separation. *Adv. Mater. Interfaces* **2018**, *5*, 1800576.

(4) Page, C. A.; Bonner, J. S.; Mcdonald, T. J.; Autenrieth, R. L. Behavior of a chemically dispersed oil in a wetland environment. *Water Res.* **2002**, *36*, 3821−3833.

(5) Zhang, T.; Li, Z.; Lü, Y.; Liu, Y.; Yang, D.; Li, Q.; Qiu, F. Recent progress and future prospects of oil-absorbing materials. *Chin. J. Chem. Eng.* **2019**, *27*, 1282−1295.

(6) Ge, J.; Zhao, H.-Y.; Zhu, H.-W.; Huang, J.; Shi, L.-A.; Yu, S.-H. Advanced Sorbents for Oil-Spill Cleanup: Recent Advances and Future Perspectives. *Adv. Mater.* **2016**, *28*, 10459−10490.

(7) Voskoboinikov, G. M.; Matishov, G. G.; Metelkova, L. O.; Zhakovskaya, Z. A.; Lopushanskaya, E. M. Participation of the Green Algae Ulvaria obscura in Bioremediation of Sea Water from Oil Products. *Dokl. Biol. Sci.* **2018**, *481*, 139−141.

(8) Adams, F. V.; Niyomugabo, A.; Sylvester, O. P. Bioremediation of Crude Oil Contaminated Soil Using Agricultural Wastes. *Procedia Manuf.* **2017**, *7*, 459−464.

(9) Nam, C. W.; Li, H. X.; Zhang, G.; Lutz, L. R.; Nazari, B.; Colby, R. H.; Chung, T. C. M. Practical oil spill recovery by a combination of polyolefin absorbent and mechanical skimmer. *ACS Sustainable Chem. Eng.* **2018**, *6*, 12036−12045.

(10) van Gelderen, L.; Malmquist, L. M. V.; Jomaas, G. Vaporization order and burning efficiency of crude oils during in-situ burning on water. *Fuel* **2017**, *191*, 528−537.

(11) Fu, B.; Yang, Q.; Yang, F. Flexible Underwater Oleophobic Cellulose Aerogels for Efficient Oil/Water Separation. *ACS Omega* **2020**, *5*, 8181−8187.

(12) Paulauskiene, T.; Uebe, J.; Karasu, A. U.; Anne, O. Investigation of Cellulose-Based Aerogels for Oil Spill Removal. *Water, Air, Soil Pollut.* **2020**, *231*, 424.

(13) Long, L.-Y.; Weng, Y. X.; Wang, Y. Z. Cellulose Aerogels: Synthesis, Applications, and Prospects. *Polymers* **2018**, *10*, 623.

(14) Su, C. P.; Yang, H.; Zhao, H. P.; Liu, Y. L.; Chen, R. Recyclable and biodegradable superhydrophobic and superoleophilic chitosan sponge for the effective removal of oily pollutants from water. *Chem. Eng. J.* **2017**, *330*, 423−432.

(15) Wang, J.; Zhao, D.; Shang, K.; Wang, Y.-T.; Ye, D.-D.; Kang, A.-H.; Liao, W.; Wang, Y.-Z. Ultrasoft gelatin aerogels for oil contaminant removal. *J. Mater. Chem. A* **2016**, *4*, 9381−9389.

(16) Cai, Y.; Wu, Y.; Yang, F.; Gan, J.; Wang, Y.; Zhang, J. Wood Sponge Reinforced with Polyvinyl Alcohol for Sustainable Oil-Water Separation. *ACS Omega* **2021**, *6*, 12866−12876.

(17) Dong, T.; Li, Q.; Nie, K.; Jiang, W.; Li, S.; Hu, X.; Han, G. Facile Fabrication of Marine Algae-Based Robust Superhydrophobic Sponges for Efficient Oil Removal from Water. *ACS Omega* **2020**, *5*, 21745−21752.

(18) Kukkar, D.; Rani, A.; Kumar, V.; Younis, S. A.; Zhang, M.; Lee, S.-S.; Tsang, D. C. W.; Kim, K.-H. Recent advances in carbon nanotube sponge-based sorption technologies for mitigation of marine oil spills. *J. Colloid Interface Sci.* **2020**, *570*, 411−422.

(19) Ieamviteevanich, P.; Palaporn, D.; Chanlek, N.; Poo-arporn, Y.; Mongkolthanaruk, W.; Eichhorn, S. J.; Pinitsoontorn, S. Carbon Nanofiber Aerogel/Magnetic Core-Shell Nanoparticle Composites as Recyclable Oil Sorbents. *ACS Appl. Nano Mater.* **2020**, *3*, 3939−3950.

(20) Li, B.; Liu, X. Y.; Zhang, X. Y.; Zou, J. C.; Chai, W. B.; Xu, J. Oil-absorbent polyurethane sponge coated with KH-570-modified graphene. *J. Appl. Polym. Sci.* **2015**, *132*, 41821.

(21) Zhou, L.; Xu, Z. Ultralight, highly compressible, hydrophobic and anisotropic lamellar carbon aerogels from graphene/polyvinyl alcohol/cellulose nanofiber aerogel as oil removing absorbents. *J. Hazard. Mater.* **2020**, *388*, 121804.

(22) Lee, J.-H.; Park, S.-J. Recent advances in preparations and applications of carbon aerogels: A review. *Carbon* **2020**, *163*, 1−18.

(23) Si, Y.; Fu, Q.; Wang, X.; Zhu, J.; Yu, J.; Sun, G.; Ding, B. Superelastic and Superhydrophobic Nanofiber-Assembled Cellular Aerogels for Effective Separation of Oil/Water Emulsions. *ACS Nano* **2015**, *9*, 3791−3799.

(24) Xu, T.; Wang, Z.; Ding, Y.; Xu, W.; Wu, W.; Zhu, Z.; Fong, H. Ultralight electrospun cellulose sponge with super-high capacity on absorption of organic compounds. *Carbohydr. Polym.* **2018**, *179*, 164−172.

(25) Lu, J.; Xu, D.; Wei, J.; Yan, S.; Xiao, R. Superoleophilic and Flexible Thermoplastic Polymer Nanofiber Aerogels for Removal of Oils and Organic Solvents. *ACS Appl. Mater. Interfaces* **2017**, *9*, 25533−25541.

(26) Shen, Y.; Li, D.; Wang, L.; Zhou, Y.; Liu, F.; Wu, H.; Deng, B.; Liu, Q. Superelastic Polyimide Nanofiber-Based Aerogels Modified with Silicone Nanofilaments for Ultrafast Oil/Water Separation. *ACS Appl. Mater. Interfaces* **2021**, *13*, 20489−20500.

(27) Jiang, G.; Ge, J.; Jia, Y.; Ye, X.; Jin, L.; Zhang, J.; Zhao, Z.; Yang, G.; Xue, L.; Xie, S. Coaxial electrospun nanofibrous aerogels for effective removal of oils and separation of water-in-oil emulsions. *Sep. Purif. Technol.* **2021**, *270*, 118740.

(28) Ge, J.; Jia, Y.; Cheng, C.; Sun, K.; Peng, Y.; Tu, Y.; Qiang, Y.; Hua, Z.; Zheng, Z.; Ye, X.; Xue, L.; Jiang, G. Polydimethylsiloxane-functionalized polyacrylonitrile nanofibrous aerogels for efficient oil absorption and oilwater separation. *J. Appl. Polym. Sci.* **2021**, *138*, 51339.

(29) Zhao, J.; Wang, F.; Zhang, X.; Liang, L.; Yang, X.; Li, Q.; Zhang, X. Vibration Damping of Carbon Nanotube Assembly Materials. *Adv. Eng. Mater.* **2018**, *20*, 1700647.

(30) Bayer, I. S. Superhydrophobic coatings from ecofriendly materials and processes: A review. *Adv. Mater. Interfaces* **2020**, *7*, 2000095.

(31) Li, L.; Rong, L.; Xu, Z.; Wang, B.; Feng, X.; Mao, Z.; Xu, H.; Yuan, J.; Liu, S.; Sui, X. Cellulosic sponges with pH responsive wettability for efficient oil-water separation. *Carbohydr. Polym.* **2020**, *237*, 116133.

(32) Turco, A.; Primiceri, E.; Frigione, M.; Maruccio, G.; Malitesta, C. An innovative, fast and facile soft-template approach for the fabrication of porous PDMS for oil-water separation. *J. Mater. Chem. A* **2017**, *5*, 23785−23793.

(33) Zhang, W.; Shi, Z.; Zhang, F.; Liu, X.; Jin, J.; Jiang, L. Superhydrophobic and superoleophilic PVDF membranes for effective separation of water-in-oil emulsions with high flux. *Adv. Mater.* **2013**, *25*, 2071−2076.

(34) Agag, T.; Takeichi, T. Synthesis and characterization of novel benzoxazine monomers containing allyl groups and their high performance thermosets. *Macromolecules* **2003**, *36*, 6010−6017.